$Bi_{1-x}Sb_x$ under high pressure: Effect of alloying on the incommensurate Bi-III type composite structure

U. Häussermann,[1] O. Degtyareva,[2] A. S. Mikhaylushkin,[3] K. Söderberg,[4] S. I. Simak,[3] M. I. McMahon,[2] R. J. Nelmes,[2] and R. Norrestam[4]

[1]*Department of Inorganic Chemistry, Stockholm University, S-10691 Stockholm, Sweden*

[2]*School of Physics and Centre for Science at Extreme Conditions, The University of Edinburgh, Edinburgh EH9 3JZ, United Kingdom*

[3]*Condensed Matter Theory Group, Physics Department, Uppsala University, S-75121 Uppsala, Sweden*

[4]*Department of Structural Chemistry, Stockholm University, S-10691 Stockholm, Sweden*

(Received 6 June 2003; revised manuscript received 12 December 2003; published 15 April 2004)

The high-pressure structural behavior of alloys $Bi_{1-x}Sb_x$ was investigated experimentally and by means of first-principles calculations in order to study the effect of alloying on the incommensurate Bi-III type composite structure, which is adopted by the high-pressure phases Bi-III and Sb-II of the pure elements. High-pressure experiments of $Bi_{0.75}Sb_{0.25}$ and $Bi_{0.50}Sb_{0.50}$ resulted in a decomposition into Sb-rich phases with the ambient A7 structure and Bi-rich phases with the Bi-III structure. For $Bi_{0.50}Sb_{0.50}$ two composite phases were observed with different compositions. $Bi_{0.25}Sb_{0.75}$ transformed from A7 to Bi-III, such as elemental Sb, and did not show a phase separation under pressure. For the pure elements, the structural parameters of the high-pressure composite phase are similar and vary only very slightly with pressure. The parameters of the alloy composite phases distribute rather smoothly in between those for the elements. The incommensurate composite phases in alloys $Bi_{1-x}Sb_x$ appear to be site disordered. Importantly, the incommensuration of the Bi-III structure is virtually not influenced by either composition or pressure. Total energy calculations as a function of pressure yielded endothermic enthalpies of formation for alloys $Bi_{1-x}Sb_x$ in both the ground-state A7 structure and the high-pressure Bi-III structure. The formation enthalpy takes a maximum value at a pressure corresponding to the alloy A7→Bi-III transition, which explains the experimentally observed phase separations.

DOI: 10.1103/PhysRevB.69.134203 PACS number(s): 61.50.Ks

I. INTRODUCTION

Recently it was discovered that Rb, Sr, Ba, and the heavier group 15 elements As, Sb, Bi adopt high-pressure structures with two interpenetrating components, a host and a guest structure, which are incommensurate with each other [Rb-IV,[1] Ba-IV,[2] Sr-V,[3] As-III, Sb-II, and Bi-III (Ref. 4)] The occurrence of a composite structure in an element, where the host and guest component are formed by the same kind of atom, is most unusual and has attracted much attention.[5] Particularly astonishing is the fact that this new type of metallic structure is found in electronically different elements from different main groups. Additionally, the high-pressure stability ranges of these incommensurate composite structures are rather extended.

The simplest composite high-pressure structure is realized in isostructural Sb-II and Bi-III (Bi-III structure type).[4] Bi and Sb possess the A7 structure as the ground state structure [cf. Fig. 1(a)].[6] Sb-II forms from Sb-I at 8.6 GPa (Refs. 4, 7, and 8) and persists to 28 GPa, where the transformation to bcc Sb-III takes place.[9] Bi-I transforms already at 2.77 GPa via the Bi-II structure into Bi-III.[10,11] Bi-III is stable up to 7.7 GPa,[4,10,12] where it is succeeded by Bi-V with the bcc structure.[13] The Bi-III structure is depicted in Fig. 1(b). It can be described by the use of two interpenetrating three-dimensional (3D) tetragonal lattices. The host component is defined by the Wyckoff site $8h$ in space group $I4/mcm$ which results in 3^2434 nets[14] stacked in an antiposition orientation along the c direction. Thus, the host structure corresponds to an assembly of rows of square antiprisms which channel linear chains of guest atoms. The guest atom arrangement corresponds to a body-centered tetragonal structure (space group $I4/mmm$) with the same a and b axes as the host. Along the c direction host and guest are incommensurate. For Bi-III and Sb-II the ratio between the two c axes, c_H/c_G, is very similar—around 1.31. The c_H/c_G ratio defines the ratio between the number of host and guest atoms in the Bi-III structure, which is 8:2.620 ($\approx 3:1$).

We performed a combined experimental and theoretical study on the high-pressure behavior of alloys $Bi_{1-x}Sb_x$. At

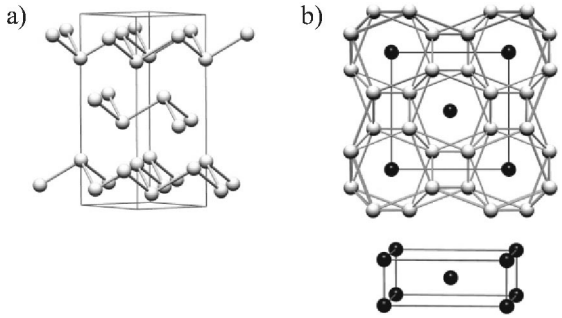

FIG. 1. (a) The rhombohedral A7 ground-state structure of Sb and Bi shown approximately along $[1\bar{1}0]$. The lines denote short intralayer atomic distances. (b) The tetragonal Bi-III structure shown along [001]. Host atoms, light gray; guest atoms, black. The guest structure, which is additionally depicted separately below, is incommensurate with the host along [001].

ambient conditions the binary system Bi-Sb forms a solid solution $Bi_{1-x}Sb_x$ with the A7 structure over the whole range of composition $0 \leqslant x \leqslant 1$. Earlier investigations of this system were performed by Bridgman (resistance measurements up to 10 GPa),[15] Akaishi and Saito (differential thermal analyses up to 4 GPa),[16] and Kolobyanina *et al.* (resistance and diffraction investigations).[17] However, the detailed high-pressure structural behavior of $Bi_{1-x}Sb_x$ is not known yet. Our particular intention was to examine how incommensuration in the Bi-III type composite is influenced when two differently sized atoms in different concentrations form the structure. In this respect, the question whether Bi and Sb atoms order on the host and guest sublattices is especially interesting. We report detailed pressure structural variations of the composite structure formed by some alloys. These variations are compared to those occurring in elemental Bi-III and Sb-II. First-principles calculations were used to model and interpret the experimental findings. The experimental and computational details are given in Secs. II and III, respectively. In Sec. IV the obtained results are presented and discussed. A summary is given in Sec. V.

II. EXPERIMENTAL DETAILS

A. Sample preparation and analysis

The alloys $Bi_{0.75}Sb_{0.25}$, $Bi_{0.50}Sb_{0.50}$, and $Bi_{0.25}Sb_{0.75}$ were prepared from granules of Bi (ABCR, 99.9999%) and Sb (ABCR, 99.999%). Stoichiometric mixtures of Bi and Sb with a sample weight of 1 g were loaded into quartz ampoules, which were sealed under vacuum. Samples were heated to 650 °C for three days and subsequently quenched in water. To obtain alloys with a homogeneous composition the fused samples were ground, pressed into pellets, and annealed for one month at temperatures 10–30 K below the $Bi_{1-x}Sb_x$ solidus curve (280, 320, and 390 °C for $x_{Sb} = 0.25$, 0.50, and 0.75, respectively).[18] The polycrystalline products were characterized by powder x-ray-diffraction patterns taken on a Guinier powder camera with Cu $K\alpha_1$ radiation ($\lambda = 1.540\,562$ Å). Lattice constants were obtained from a least-square refinement of the indexed lines using Si (NIST) as internal standard.[19] Elemental composition was determined by the energy disperse x-ray (EDX) method in a JEOL scanning microscope by averaging analyses of at least ten different crystallites from each sample. The result of the EDX analysis was $Bi_{0.75}Sb_{0.25}$, $x_{Sb} = 0.219(7)$, $Bi_{0.50}Sb_{0.50}$, $x_{Sb} = 0.487(7)$, and $Bi_{0.25}Sb_{0.75}$, $x_{Sb} = 0.749(8)$. For obtaining $Bi_{1-x}Sb_x$($x_{Sb} = 0.25$, 0.50, and 0.75) crystals with suitable size for single-crystal high-pressure investigations, synthesis conditions had to be modified. Samples were prepared with an excess of Bi and the synthesis temperature was chosen to correspond to the respective solidus temperatures of the desired compositions (290, 335, and 420 °C for $x_{Sb} = 0.25$, 0.50, and 0.75, respectively).[18] Under these conditions solid alloy is in equilibrium with a Bi-richer melt, which is very favourable for crystal growth. Reaction times were 3–4 days and alloy crystals were subsequently separated from the melt by centrifugation. The result of the compositional analysis for these products was $Bi_{0.75}Sb_{0.25}$, $x_{Sb} = 0.218(8)$, $Bi_{0.50}Sb_{0.50}$, $x_{Sb} = 0.520(9)$, and $Bi_{0.25}Sb_{0.75}$, $x_{Sb} = 0.74(1)$. In summary, we succeeded in the preparation of homogeneous polycrystalline and single crystalline samples $Bi_{1-x}Sb_x$. However, their compositions deviated slightly from the nominal ones. Nevertheless, in the following we denote the alloys with their idealized composition $x_{Sb} = 0.25$, 0.50, and 0.75.

B. High-pressure experiments

Powdered samples of $Bi_{0.75}Sb_{0.25}$, $Bi_{0.50}Sb_{0.50}$, and $Bi_{0.25}Sb_{0.75}$ were loaded with methanol-ethanol (4:1) as a pressure medium and a small ruby crystal for pressure measurement in a Merril-Basset type of diamond anvil cell (DAC). Angle-dispersive powder-diffraction data were collected on station 9.1 at the Synchrotron Radiation Source, Daresbury Laboratory (UK), using an image-plate area detector, with a wavelength of $\lambda = 0.4654(1)$ Å.[20] The 2D images were integrated azimuthally and the obtained data used for Rietveld refinement of structural parameters. The resolution of data was 0.015 ° and the 2θ range covered 2 °–27 °.

Single-crystal high-pressure investigations on $Bi_{0.75}Sb_{0.25}$, $Bi_{0.50}Sb_{0.50}$, and $Bi_{0.25}Sb_{0.75}$ were performed using a Merril-Basset type of DAC with diamond culet diameters of 0.6 mm. Crystal sizes were about $0.10 \times 0.10 \times 0.03$ mm^3. A mixture of methanol-ethanol-water (16:3:1) served as pressure medium and the ruby R_1 fluorescence line shift was used for pressure calibration.[21] Diffraction data were collected using Mo $K\alpha$ radiation from a rotating anode x-ray generator with a four-circle diffractometer (Siemens P4/RA). Cell parameters were determined from positions of 12–19 well centred reflections with $2 < 2\theta < 31°$.

All high-pressure experiments were performed at room temperature and the results reported in this work stem exclusively from ascending pressure runs.

C. Structure refinements

The refinements of structural parameters from the powder-diffraction profiles ($Bi_{1-x}Sb_x$ and earlier collected Bi and Sb, Ref. 5) were performed with the current version of the program JANA2000 for Linux.[22] This software package provides an easy handling of profile refinements of powder data from multiphase incommensurate samples (including multiphase composites). The profiles were described by pseudo-Voigt functions and the backgrounds were described by fitting them to seven terms Legendre polynoms.

Previously, the diffraction pattern of high-pressure Bi-III and Sb-II was described by the use of two interpenetrating 3D tetragonal lattices.[4] However, after the completion of the present study single crystal diffraction data from elemental Bi-III could be obtained and a structure refinement in 4D superspace group symmetry performed.[23,24] Interestingly, this refinement revealed a rather strong modulation of the guest component leading to a quasipairing of atoms in the channels defined by the square antiprisms of host atoms [cf. Fig. 1(b)]. Also the host atom arrangement showed a weak modulation, which might be interpreted as a response to the much stronger guest atom modulation.[25] The 4D superspace

group $X4/mcc(00\gamma)$ with the centering vector $(\frac{1}{2},\frac{1}{2},\frac{1}{2},\frac{1}{2})$ can be used for the modulation vector $\mathbf{q}^*=\gamma\cdot\mathbf{c}_H^*\approx 1.31\mathbf{c}_H^*$ in order to describe the diffraction pattern of the composite structure. Consequently, it is indexed using 4 integers (h,k,l,m) according to

$$\mathbf{d}_{hklm}^*\equiv h\mathbf{a}^*+k\mathbf{b}^*+l\mathbf{c}^*+m\mathbf{q}^*.$$

However, the use of one of the conventional superspace group symmetries as listed by Janssen *et al.* in Ref. 27 appears more advantageous. Instead of the longer $\approx 1.31\mathbf{c}_H^*$ used above, the shorter vector $\mathbf{q}^*\approx 0.31\mathbf{c}_H^*$ is selected. For this case the superspace group $I4/mcm(00\gamma)00ss$ is applicable and will be used throughout the present study.

In the space group $I4/mcm(00\gamma)00ss$, the host atoms of the Bi-III type occupy the eightfold position $(x,1/2+x,0)$ with $x\approx 0.154$ and the guest atoms the twofold position (0,0,0). In the Rietveld refinements of structural parameters of alloys $Bi_{1-x}Sb_x$ with the Bi-III structure we observed that generally better fits were obtained when assuming that the guest atoms were positionally modulated. This accords with the above described situation in elemental Bi-III. The tetragonal *I* symmetry restriction implies that there is only one parameter required to describe a positional modulation up to the second order. Some very minor peak positions in the low angle region of the diffraction pattern were in accordance with satellite positions due to a guest atom modulation. To describe a positional modulation of the host atoms up to second order, three independent parameters are needed. Initial refinements including a host atom modulation did not converge properly due to insufficient information in the powder-diffraction data. Conclusively, the final refinements included second-order positional modulation parameters for the guest atoms. However, the modulation amplitudes have limited statistical relevance because of the lack of relevant information in some of the data sets.

The detailed refinement results are extensive and cannot be presented in full length. However, we provide seven tables as supplementary information:[37] Tables S-I, S-II, and S-III of Ref. 37 contain the Rietveld refinement results for the different alloys, and Tables S-IV and S-V those for the pure elements. Table S-VI lists the unit-cell parameters obtained from single crystal high-pressure measurements and Table S-VII displays the unit cell parameters at ambient condition.

III. COMPUTATIONAL DETAILS

Total energy calculations for $Bi_{0.75}Sb_{0.25}$, $Bi_{0.50}Sb_{0.50}$, and $Bi_{0.25}Sb_{0.75}$ as a function of pressure were performed in the framework of the frozen core scalar-relativistic all-electron projected augmented wave method,[28] as implemented in the program VASP.[29] The alloys were considered in the structure types A7 and Bi-III. The energy cutoff was set to 300 eV. Exchange and correlation effects were treated by the generalized gradient approximation,[30] usually referred to as PW91. The integration over the Brillouin zone was done on special *k* points determined according to the Monkhorst-Pack scheme.[31] All necessary convergency tests were performed and total energies were converged to 0.1 meV/atom.

Conventional electronic structure calculations are based on periodic boundary conditions. Therefore, an incommensurate structure has to be approximated by a supercell. The proximity of c_H/c_G to the commensurate ratio $4/3=1.333$ suggests that the Bi-III structure can be modeled by a commensurate supercell with a trebled host *c* axis. Thus, the unit cell of the model structure used in our calculations contained 24 host atoms in six 3^2434 nets and eight body-centered tetragonal guest atoms in the channels along (0,0,z) and $(\frac{1}{2},\frac{1}{2},z)$. The ratio between host and guest atoms in the model structure is 8:2.667 which implies that its density is slightly higher compared with that of the experimental structure. A detailed description of the Bi-III type model structure can be found in Ref. 32. With this model structure we were able to reproduce the experimentally established pressure stability ranges of the host-guest structure for elemental Bi and Sb extremely well.

Bi/Sb site disorder in the alloys was modeled with the help of special quasirandom structures[33] which mimic random atomic distribution for several coordination shells in a supercell. The supercell for the rhombohedral A7 structure contained 12 atoms and was chosen on the basis of the A7 hexagonal unit cell which was doubled by $a_{ortho}=a_{hex}$, $b_{ortho}=\sqrt{3}b_{hex}$, and $c_{ortho}=c_{hex}$. The supercell for the tetragonal Bi-III structure corresponded to the supercell approximating the incommensurate c_H/c_G ratio (32 atoms). The atomic position parameters and lattice parameters of the supercells were relaxed for a set of constant volumes until forces had converged to less than 0.01 eV/Å. During the relaxation procedure the lattices of the supercells were constrained to be orthorhombic and tetragonal for A7 and Bi-III, respectively, although the symmetry of the cell content is triclinic for randomly disordered alloys. In a second step we fitted the *E* vs *V* values of all structures by cubic splines and obtained the pressure vs volume dependence through a very accurate numerical differentiation of *E* with respect to *V*. After having obtained the pressure, enthalpies H were calculated according to $H(p)=E(p)+pV(p)$.

IV. RESULTS AND DISCUSSION

A. Experimental results

At ambient conditions Bi, Sb, and the alloys $Bi_{0.75}Sb_{0.25}$, $Bi_{0.50}Sb_{0.50}$, and $Bi_{0.25}Sb_{0.75}$ possess the rhombohedral A7 structure [space group $R\bar{3}m$, Fig. 1(a)]. When specifying the A7 structure with hexagonal axes the structural parameters are the c/a ratio and the *z* parameter of the Wyckoff position $6c(0,0,z)$. For Bi, Sb, and the three prepared alloys c/a ratio and *z* parameter are very similar, around 2.62 and 0.234, respectively. The unit-cell volume for $Bi_{1-x}Sb_x$ increases almost linearly with increasing Bi content, which is shown in Fig. 2. We recall that the A7→Bi-III transition occurs at 2.8 and 8.6 GPa for Bi and Sb, respectively. The results of the high-pressure investigation on $Bi_{0.25}Sb_{0.75}$, $Bi_{0.50}Sb_{0.50}$, and $Bi_{0.75}Sb_{0.25}$ are shown as plots of the atomic volumes vs pressure in Fig. 3. Data from powder and single-crystal in-

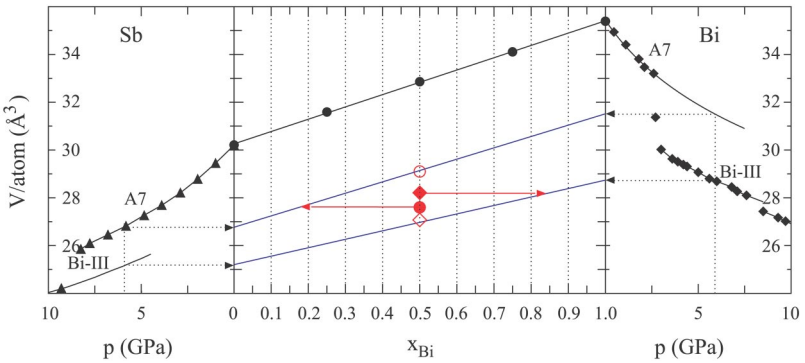

FIG. 2. (Color online) Atomic volumes of the Bi-Sb alloy phases vs composition (middle) and atomic volume of pure elements Sb (left) and Bi (right) vs pressure. Atomic volumes of the A7 phases in Bi-Sb alloys at ambient conditions are shown by solid circles and fitted with a straight line. The colored symbols denote observed atomic volumes of the occurring four phases in $Bi_{0.50}Sb_{0.50}$ at 5.9 GPa: $A7_1$ (open red circle), $A7_2$ (filled red circle), Bi-III_1 (filled red diamond), and Bi-III_2 (open red diamond). The atomic volumes of pure elements at these pressures are extracted from the *p-V* curves (dotted arrows), and the compositions of the $Bi_{0.50}Sb_{0.50}$ alloy phases are estimated at these pressures (solid red arrows) from the linear interpolation between the atomic volumes of pure elements (solid blue lines). This procedure has been applied for the determination of phase compositions in multiphase specimens as presented in Table I

vestigations are combined. Additionally, this figure includes the compression data of the pure elements for comparison.

Structural transitions. For $Bi_{0.25}Sb_{0.75}$ at 6.6(3) GPa the initial A7 phase starts to transform into the high-pressure Bi-III phase. The A7 and Bi-III phases coexist up to 7.7 GPa. Thus, the A7→Bi-III transition of $Bi_{0.25}Sb_{0.75}$ is sluggish in contrast to the sharp transition occurring in pure Sb.

For $Bi_{0.50}Sb_{0.50}$ the single-crystal studies showed that when keeping a single crystal of an A7 specimen in the DAC at 4.5 GPa for several hours, it eventually undergoes a phase transition to a polycrystalline specimen. The powder-diffraction studies confirm that the initial A7 phase ($A7_1$) is partially transformed at about 4.5 GPa into a Sb-rich A7 phase ($A7_2$) and a Bi-rich composite Bi-III phase (Bi-III_1). The $A7_1$ phase is observed up to at least 5.9 GPa and the Sb-rich $A7_2$ phase up to 8.4 GPa. When roughly estimating compositions from a linear interpolation of elemental atomic volumes (as explained in Fig. 2) the x_{Sb} values for $A7_2$ and Bi-III_1 are about 0.82 and 0.17, respectively (cf. Table I). At 5.9 GPa a second Bi-III phase (Bi-III_2) with an estimated composition $x_{Sb}=0.50$ (cf. Fig. 2, Table I) is observed. The Rietveld refined diffraction profile at this pressure is shown in Fig. 4. Bi-III_2 should result from a transformation $A7_1$ →Bi-III_2; the phase fraction of $A7_1$ at 5.1 GPa (56%) and Bi-III_2 at 5.9 GPa (47%) appear to be correlated.

For $Bi_{0.75}Sb_{0.25}$ the single-crystal studies showed that when keeping a single crystal of an A7 specimen in the DAC at 3.41 GPa for several hours, it eventually undergoes a phase transition to a polycrystalline specimen. The powder-diffraction studies confirm that the initial A7 structure ($A7_1$) is transformed at about 3.4 GPa into a Bi-rich major phase with the composite Bi-III structure and a Sb-rich minor phase with the A7 structure, denoted $A7_2$. The estimated compositions (cf. Fig. 2, Table I) are about $x_{Sb}=0.82$ for $A7_2$ and $x_{Sb}=0.12$ for Bi-III. The $A7_2$ phase is observed up to 7.4 GPa. Above this pressure up to 11.1 GPa the only observed phase is the composite Bi-III phase.

Phase separation. For the alloys with $x_{Sb}=0.25$ and 0.50 the A7 ambient phase decomposes into Sb-rich and Bi-rich phases. For $x_{Sb}=0.50$ two composite phases are formed with different compositions. $Bi_{0.25}Sb_{0.75}$ does not decompose and exhibits a transformation from A7 to Bi-III-like pure Sb. A decomposition of alloys $Bi_{1-x}Sb_x$($x=0.1,0.2,0.3,0.4$) was also observed in the high-pressure differential thermal analysis investigations by Akaishi and Saito.[16]

In Table I we show the estimated compositions of the different phases in some multi-phase specimens. The estimation procedure is presented in Fig. 2. First, we note that for $x_{Sb}=0.75$ there is no phase separation in the two-phase region between 6.6 and 7.7 GPa. The compositions of the coexisting A7 and Bi-III phase correspond to the sample composition. For complex $Bi_{0.50}Sb_{0.50}$ the compositions of the $A7_2$ and Bi-III_1 phase are around $x_{Sb}=0.82$ and 0.18, respectively, and that of the $A7_1$ and Bi-III_2 phase around 0.5. The estimated compositions of the different phases appear to be stable in the investigated pressure region. When taking into account the corresponding refined phase fractions the overall sample composition is obtained to a good approximation.[34] For $Bi_{0.75}Sb_{0.25}$ the compositions of the $A7_2$ and Bi-III phases are about $x_{Sb}=0.82$ and 0.12, respectively, in the pressure range between 4 and 7 GPa, i.e., as long as the $A7_2$ phase is present. At around 7 GPa $A7_2$ does not transform to a second Bi-III phase but appears to react with the present Bi-III phase, which unambiguously changes composition from $x_{Sb}=0.12$ to 0.25. This is also clearly seen in the atomic volume vs pressure plot in Fig. 3.

The observed phase separation in $Bi_{1-x}Sb_x$ poses several questions. The compositions of the A7 and Bi-III phases resulting from the separation in $Bi_{0.75}Sb_{0.25}$ and $Bi_{50}Sb_{50}$ are very similar. However, in the former alloy $A7_2$ disappears at around 7 GPa, which coincides with the expected transition pressure, whereas in the latter alloy $A7_2$ persists to 8.4 GPa. Second, for $Bi_{50}Sb_{50}$ only a part of the sample undergoes the initial phase separation; between 4.5 and 8.4 GPa a complex mixture of phases is obtained which implies a nonequilibrium situation. This at the first sight contradictory behavior might be explained by the findings of Bridgman who investigated the resistance of $Bi_{1-x}Sb_x$ under pressure up to 10

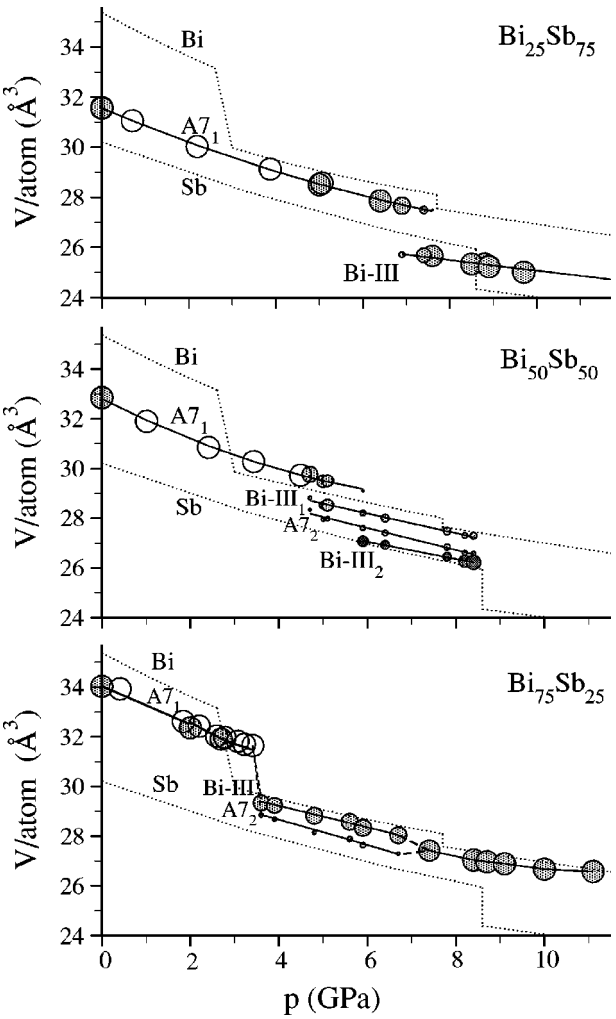

FIG. 3. Atomic volumes (Å^3) for (a) $Bi_{0.25}Sb_{0.75}$, (b) $Bi_{0.50}Sb_{0.50}$, and (c) $Bi_{0.75}Sb_{0.25}$ as a function of pressure. The empty circles denote observations by single-crystal diffractometry and the shaded ones those obtained by powder diffraction. The average atomic volumes for the composites were estimated as $V_{cell}/(10+2\gamma)$. In the multiphase regions the circles representing each phase have radii proportional to their relative fractions.

GPa already some 50 years ago.[15] He presented his data in a table from which we assembled Fig. 5. For compositions $x_{Sb} \leqslant 0.2$ there is a sharp A7→Bi-III transition at 2.8 GPa. The pressure of this transition is virtually independent from composition, which suggests a phase separation. From $x_{Sb} = 0.3$ the transition gets pushed to higher pressures and becomes smeared out. Bridgman assumed that up to $x_{Sb} = 0.2$ $Bi_{1-x}Sb_x$ is in a state of complete internal equilibrium under pressure. The conditions become increasingly nonequilibrium when the Sb content is risen until $x_{Sb} = 1$. If this applies, our sample $Bi_{0.75}Sb_{0.25}$ should have been close to internal equilibrium during the performed high-pressure experiment. This is supported by the constant phase fractions of $A7_2$ and Bi-III (cf. Table I) and explains the disappearance of $A7_2$ at the expected transition pressure. A nonequilibrium situation is clearly encountered in our $Bi_{50}Sb_{50}$ experiment where the decomposition occurred only partially. Then it appears likely that the phase separation actually should also occur in $Bi_{0.25}Sb_{0.75}$ but is completely suppressed by the increased nonequilibrium situation experienced at this high Sb content.

Finally, in Fig. 6 we sketch a pressure-composition diagram for $Bi_{1-x}Sb_x$ based on all performed experiments (cf. Tables S-I, S-II, and S-III of Ref. 34). The high-pressure structural sequence of the alloys is clearly A7→Bi-III →bcc, although for $x_{Sb} = 0.50$ we have not measured until a transition Bi-III→bcc. We note that in $Bi_{0.75}Sb_{0.25}$ also the transition Bi-III→bcc is accompanied by a phase separation, the bcc phase being Bi rich. The transition Bi-I→Bi-II, which occurs in elemental Bi, is not observed in the alloys here investigated. This transition is rapidly suppressed upon Sb alloying. Bridgman found that in $Bi_{1-x}Sb_x$ the Bi-II high-pressure phase already disappeared for x_{Sb} values as low as 0.04.[15]

Structural variations in the Bi-III type phases. The initial intention of our work was the study of the structural variations in the incommensurate Bi-III structure as a function of pressure and composition. The tetragonal composite structure [cf. Fig. 1(b)] is described by three structural parameters: the c/a ratio of the host component (c_H/a_H), the positional parameter x of the host atoms occupying the Wyckoff site $8h$ $(x,x+\frac{1}{2},0)$, and the incommensurate ratio between the c axes of the host and guest component (c_H/c_G). The latter is equivalent to the magnitude of the modulation vector $(1+\gamma)\mathbf{c}_H^*$. We compiled the pressure variations of the structural parameters of the Bi-III type phases of the pure elements and alloys $Bi_{1-x}Sb_x$ in Fig. 7. We recall that our experiments yielded Bi-III type alloys with five significantly different compositions (Bi-III in $Bi_{0.25}Sb_{0.75}$, $Bi\text{-}III_1$ and $Bi\text{-}III_2$ in $Bi_{0.5}Sb_{0.5}$, and Bi-III with altered composition in $Bi_{0.75}Sb_{0.25}$).

It is clearly seen that the γ values (≈ 0.31) of the modulation vector $\gamma\mathbf{c}_H^*$ change only slightly [cf. Fig. 7(a)]. By omitting the results for specimens containing two different composite phases (i.e., the $Bi_{50}Sb_{50}$ data) which are likely to be less accurate due to possible correlation problems, there is a pronounced trend that the γ values decrease slightly with pressure (from about 0.3115 to 0.3075). No significant correlation of γ values with composition is observed. The c_H/a_H ratios for the composite phases [cf. Fig. 7(b)] decrease slightly with pressure. There is a clear correlation between c_H/a_H values and composition. Thus, the c_H/a_H values, which range from about 0.489 (pure Bi) to about 0.484 (pure Sb), decrease with increasing x_{Sb}. Also the positional parameter of the composite phases is rather constant. A small increase of the positional composite phase x parameter with increasing Sb content can be observed as indicated in Fig. 7(c). The values range from about 0.153 (pure Bi) to 0.156 (pure Sb). With pressure the x parameters of the composite phases show an almost insignificant small decrease with pressure. In pure Sb, where the composite phase has the largest pressure stability range, the value decreases from 0.1566 at 10.2 GPa to 0.1544 at 25.6 GPa. We should note that the highly textured Bi powder-diffraction patterns did not allow a reliable refinement of the x parameter. Figure 7(c) shows only the results at 6.8 and 7.6 GPa, where R_{bragg} values

TABLE I. Estimated compositions and refined fractions of the different phases occurring in selected multiphase specimens $Bi_{0.50}Sb_{0.50}$ and $Bi_{0.75}Sb_{0.25}$ under pressure.

Sample	p (GPa)	Phases	Estimated composition	Fraction	Total composition
$Bi_{0.25}Sb_{0.75}$	6.9	A7	$Bi_{0.25}Sb_{0.75}$	0.774(5)	$Bi_{0.25}Sb_{0.75}$
		Bi-III	$Bi_{0.25}Sb_{0.75}$	0.226(5)	
$Bi_{0.50}Sb_{0.50}$	5.0	$A7_1$	$Bi_{0.49}Sb_{0.51}$	0.560(7)	$Bi_{0.52}Sb_{0.48}$
		$A7_2$	$Bi_{0.16}Sb_{0.84}$	0.166(6)	
		$Bi\text{-}III_1$	$Bi_{0.83}Sb_{0.17}$	0.274(4)	
	5.9	$A7_1$	$Bi_{0.50}Sb_{0.50}$	0.046(3)	$Bi_{0.49}Sb_{0.51}$
		$A7_2$	$Bi_{0.18}Sb_{0.82}$	0.219(2)	
		$Bi\text{-}III_1$	$Bi_{0.83}Sb_{0.17}$	0.261(4)	
		$Bi\text{-}III_2$	$Bi_{0.50}Sb_{0.50}$	0.474(6)	
	6.4	$A7_1$	$Bi_{0.50}Sb_{0.50}$	0.008(1)	$Bi_{0.51}Sb_{0.49}$
		$A7_2$	$Bi_{0.18}Sb_{0.82}$	0.260(4)	
		$Bi\text{-}III_1$	$Bi_{0.82}Sb_{0.18}$	0.350(4)	
		$Bi\text{-}III_2$	$Bi_{0.50}Sb_{0.50}$	0.382(6)	
	7.8	$A7_2$	$Bi_{0.15}Sb_{0.85}$	0.282(3)	$Bi_{0.51}Sb_{0.49}$
		$Bi\text{-}III_1$	$Bi_{0.82}Sb_{0.18}$	0.339(3)	
		$Bi\text{-}III_2$	$Bi_{0.52}Sb_{0.48}$	0.379(5)	
$Bi_{0.75}Sb_{0.25}$	4.8	$A7_2$	$Bi_{0.18}Sb_{0.82}$	0.236(6)	$Bi_{0.72}Sb_{0.28}$
		$Bi\text{-}III_1$	$Bi_{0.89}Sb_{0.11}$	0.764(6)	
	5.6	$A7_2$	$Bi_{0.20}Sb_{0.80}$	0.238(6)	$Bi_{0.72}Sb_{0.28}$
		$Bi\text{-}III_1$	$Bi_{0.88}Sb_{0.12}$	0.762(6)	
	5.9	$A7_2$	$Bi_{0.18}Sb_{0.82}$	0.225(6)	$Bi_{0.73}Sb_{0.27}$
		$Bi\text{-}III_1$	$Bi_{0.89}Sb_{0.11}$	0.775(6)	
	6.7	$A7_2$	$Bi_{0.20}Sb_{0.80}$	0.225(6)	$Bi_{0.73}Sb_{0.27}$
		$Bi\text{-}III_1$	$Bi_{0.89}Sb_{0.11}$	0.775(6)	
	8.4	$Bi\text{-}III_2$	$Bi_{0.75}Sb_{0.25}$	1.000	$Bi_{0.75}Sb_{0.25}$
	10.0	$Bi\text{-}III_2$	$Bi_{0.75}Sb_{0.25}$	1.000	$Bi_{0.75}Sb_{0.25}$

around or below 0.1 could be obtained (cf. Table S-IV of Ref. 34). Additionally, the value from a single-crystal refinement at 5.5 GPa is included.[24] For $x_{Sb}=0.25$ the change in composition of the Bi-III phase after the disappearance of $A7_1$ (at 7 GPa) is clearly recognizable in the altered values for c_H/a_H and the x parameter. In conclusion, apart from the unit-cell compression, the structural parameters of the phases with the composite structure are remarkably unaffected by pressure and composition effects.

An interesting question concerning the Bi-III structure in alloys $Bi_{1-x}Sb_x$ is whether Bi and Sb atoms order on the host and guest sublattices. The fact that the structural param-

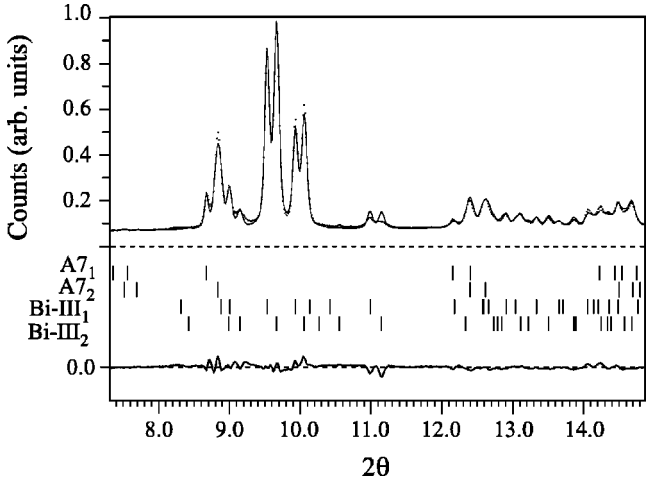

FIG. 4. Integrated powder-diffraction profile from the four-phase specimen $Bi_{0.50}Sb_{0.50}$ at 5.9 GPa (dots) and a Rietveld refinement fit (line) ($R_{profile}=3.7\%$, $R_{bragg,A7_1}=4.1\%$, $R_{bragg,A7_2}=3.2\%$, $R_{bragg,\mathrm{Bi}-III_1}=3.6\%$, $R_{bragg,\mathrm{Bi}-III_2}=4.5\%$).

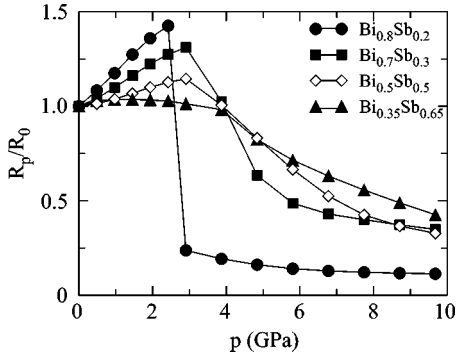

FIG. 5. Resistance as a function of pressure (R_p) normalized to the resistance at ambient conditions (R_0) of alloys $Bi_{1-x}Sb_x$ [$x=0.2$ (circles), 0.3 (squares), 0.5 (diamonds), 0.65 (triangles)] according to Bridgman (Ref. 15).

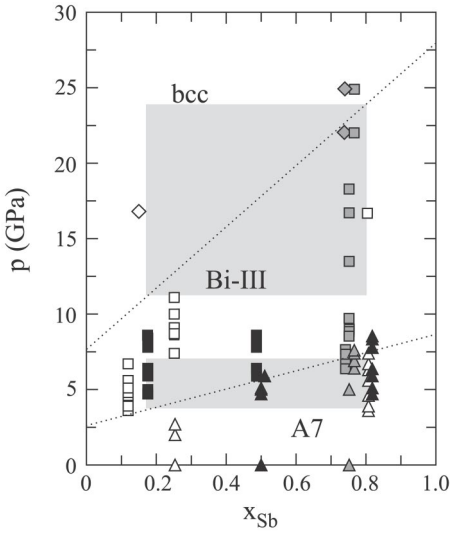

FIG. 6. Sketch of a p vs x phase diagram for $Bi_{1-x}Sb_x$ based on all performed experiments (at room temperature). White, black, and gray symbols distinguish the results for $Bi_{0.75}Sb_{0.25}$, $Bi_{0.50}Sb_{0.50}$, and $Bi_{0.25}Sb_{0.75}$, respectively (triangles, A7; squares, Bi-III; diamonds, bcc). Note that the compositions in phase separated samples are just estimated (cf. Fig. 2). The dotted lines connect experimentally observed transition pressures in the pure elements and, thus, only approximate the phase boundaries. Possible thermodynamic miscibility gaps are indicated by light gray areas.

eters of the alloy composite phases distribute smoothly in between those for the pure elements indicates that Bi and Sb atoms are randomly distributed on the host and guest structures. However, the compositions of the Bi-III phase obtained in the $Bi_{0.25}Sb_{0.75}$ and the $Bi_{0.75}Sb_{0.25}$ experiment above 7 GPa would allow for complete host-guest ordering (i.e., a Sb host and a Bi guest for the former and vice versa for the latter). In the initial refinements of the Bi-III specimens the compositions at the host and guest positions were refined, under the constraint that their sum was fixed to the estimated phase composition (Table I). No indication of a different composition was obtained in any of the cases studied. Similarly, we refined the occupancy at the guest site while keeping the compositions at the host and guest positions fixed. In no case the occupancies obtained deviated by more than a few standard deviations (e.s.d.'s) from 100%. We therefore conclude that the Bi-III structure observed in alloys $Bi_{1-x}Sb_x$ is site disordered.

B. Computational results

A7→Bi-III transition. We calculated enthalpy differences A7→Bi-III for $Bi_{1-x}Sb_x$ ($x=0.0,0.25,0.50,0.75,1.0$). The results are displayed in Fig. 8. The extracted transition pressures are 3.6, 4.3, 5.1, 6.7, and 9.0 GPa. The calculated transition pressure for Sb is in good agreement with the room temperature experiment (8.6 GPa). Concerning Bi there is no direct transition A7→Bi-III at room temperature. The first structural high-pressure transition at 2.55 GPa results in monoclinic Bi-II which has a very narrow stability range: at 2.77 GPa the transformation to tetragonal Bi-III takes place.

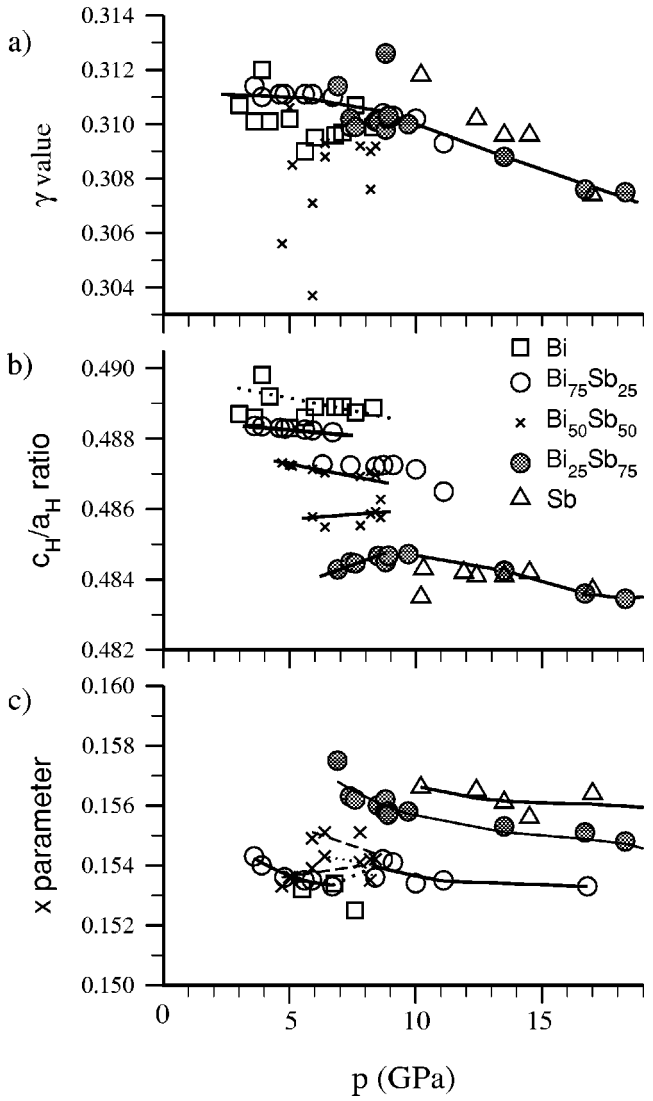

FIG. 7. Structural variations of the composite Bi-III structure as a function of composition and pressure: (a) γ value, (b) c_H/a_H axial ratio, (c) the fractional x positional parameter of the site $8h$ in space group $I4/mcm$. Pure Bi, squares; $Bi_{0.75}Sb_{0.25}$, empty circles; $Bi_{0.50}Sb_{0.50}$, crosses; $Bi_{0.25}Sb_{0.75}$, shaded circles; and pure Sb, triangles. The values for the composition $x_{Sb}=0.50$, for which two composite phases occur simultaneously, are likely to be less accurate due to correlation problems.

The Bi-II stability range decreases with decreasing temperature and vanishes at about 200 K. Theoretical calculations yield a direct A7→Bi-III transition.[32] The calculated A7→Bi-III transition pressures for $x_{Sb}=0.25$, 0.50, and 0.75 agree reasonably with the experimentally observed high-pressure structural changes at 3.4, 4.5, and 6.6 GPa, respectively.

The transformation A7→Bi-III in $Bi_{1-x}Sb_x$ corresponds to a semimetal-metal transition. We show in Fig. 9 the electronic density of states (DOS) of Bi, Sb, and $Bi_{0.50}Sb_{0.50}$ in the A7 and Bi-III structure close to the respective transition pressures. The DOS resulting from the A7 structure can be divided into four parts: *s-s* bonding, *s-s* antibonding, *p-p* bonding, and *p-p* antibonding. The Fermi level is located

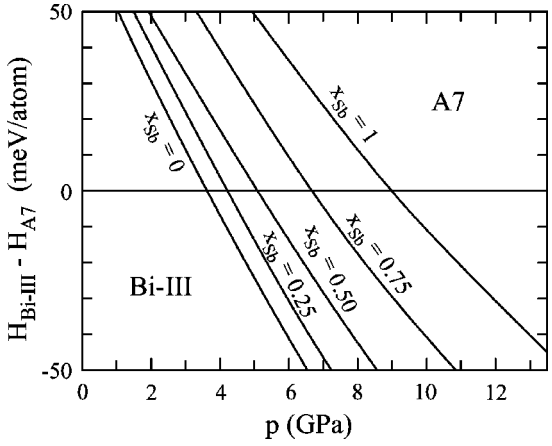

FIG. 8. Calculated enthalpy differences ΔH (Bi-III-A7) for $Bi_{1-x}Sb_x$ ($x=0,0.25,0.50,0.75,1$) as a function of pressure.

between the *p-p* bonding and antibonding bands in a deep pseudo gap with a very low value of density of states. For the Bi-III type phases the overall shape of the DOS curves recall that of the corresponding A7 ones. However, the density of states at the Fermi level is drastically increased and the deep pseudogap which separated *p-p* bonding from antibonding states in the A7 DOS has changed into a shallow, although marked, well. The persistence of the *p* band bonding-antibonding splitting indicates a still significant covalent *p-p* bonding in the host-guest structure. Thus, the structural transition A7→Bi-III in $Bi_{1-x}Sb_x$ is accompanied with a rather smooth variation in the electronic structure.

Phase separation. In order to investigate the experimentally observed phase separation of $Bi_{1-x}Sb_x$ under pressure we assembled the enthalpies of the following reactions:

$$(1-x)\mathrm{Bi(A7)}+x\ \mathrm{Sb(A7)}\rightarrow \mathrm{Bi}_{1-x}\mathrm{Sb}_x\mathrm{(A7)}, \quad (1)$$

$$(1-x)\mathrm{Bi(Bi\text{-}III)}+x\ \mathrm{Sb(A7)}\rightarrow \mathrm{Bi}_{1-x}\mathrm{Sb}_x\mathrm{(A7)}, \quad (2)$$

$$(1-x)\mathrm{Bi(Bi\text{-}III)}+x\ \mathrm{Sb(A7)}\rightarrow \mathrm{Bi}_{1-x}\mathrm{Sb}_x\mathrm{(Bi\text{-}III)}, \quad (3)$$

$$(1-x)\mathrm{Bi(Bi\text{-}III)}+x\ \mathrm{Sb(Bi\text{-}III)}\rightarrow \mathrm{Bi}_{1-x}\mathrm{Sb}_x\mathrm{(Bi\text{-}III)}. \quad (4)$$

These alloy formation enthalpies are shown as a function of pressure in Fig. 10. If we first focus on the situation at ambient pressure, we observe that the formation of $Bi_{1-x}Sb_x$ (A7) alloys is endothermic (i.e., energetically unfavorable) with about 11 meV/atom for $x_{Sb}=0.25$ and 0.75 [cf. Figs. 10(a) and 10(c)], and about 15 meV/atom for $x_{Sb}=0.50$ [Fig. 10(b)]. This compares surprisingly well with measured mixing enthalpies, which are in a range of 1 to 1.5 kJ/g mol.[35] Above the A7→Bi-III transition pressure for elemental Bi (at 3.6 GPa) reaction (2) should be considered, which makes the alloy formation even more endothermic. A maximum value of formation enthalpy occurs at the alloy A7→Bi-III transition pressure, where reaction (2) is succeeded by reaction (3). The first experimentally observed transition for each investigated alloy occurs at a pressure close to the corresponding calculated A7→Bi-III transition pressure. Therefore, we assume that the phase separation observed in our experiment does not occur until the A7→Bi-III transition pressure for the alloy is reached. At that point a separation into a Sb-rich A7 phase ($x_{Sb}=0.80$–0.85) and a Bi-rich Bi-III phase ($x_{Sb}=0.10$–0.20) takes place [reaction (3)]. According to our calculations the separation should also have been observed for $Bi_{0.25}Sb_{0.75}$. This phase separation is not observed in our $Bi_{0.25}Sb_{0.75}$ experiment. However, as already discussed in the preceding section the decomposition is probably suppressed by the increased state of nonequilibrium encountered for higher Sb contents. Finally, the reaction of Sb-rich $A7_2$ with Bi-rich Bi-III (reverse phase separation) occurring at 7 GPa in $Bi_{0.75}Sb_{0.25}$ (where internal equilibrium can be assumed) is plausible from the considerably lowered formation enthalpy at this pressure, which becomes comparable to that at ambient pressure [Fig. 10(a)]. Provided complete internal equilibrium we propose a miscibility gap for the binary system $Bi_{1-x}Sb_x$ under pressure (at room temperature). This gap is

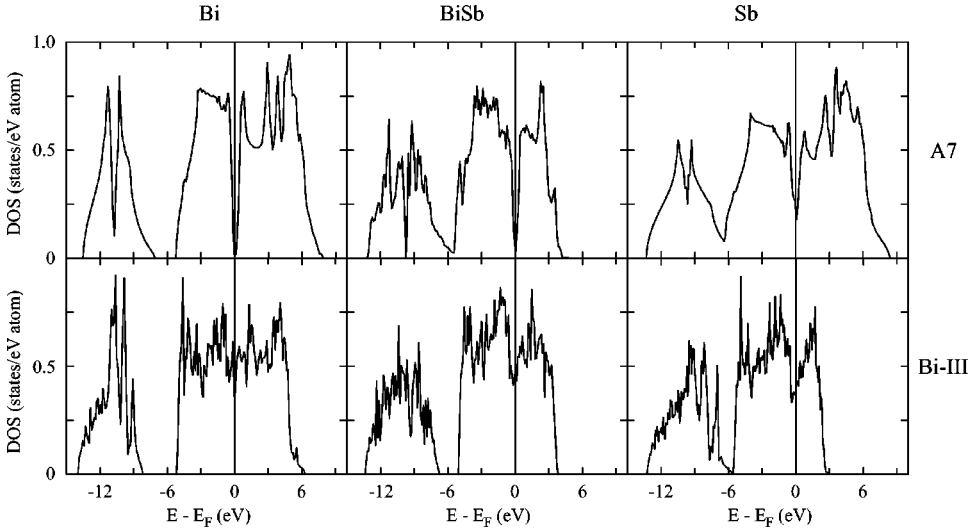

FIG. 9. Density of states (DOS) of Bi, $Bi_{0.50}Sb_{0.50}$, and Sb in the A7 and Bi-III structures at volumes close to the respective transition pressures.

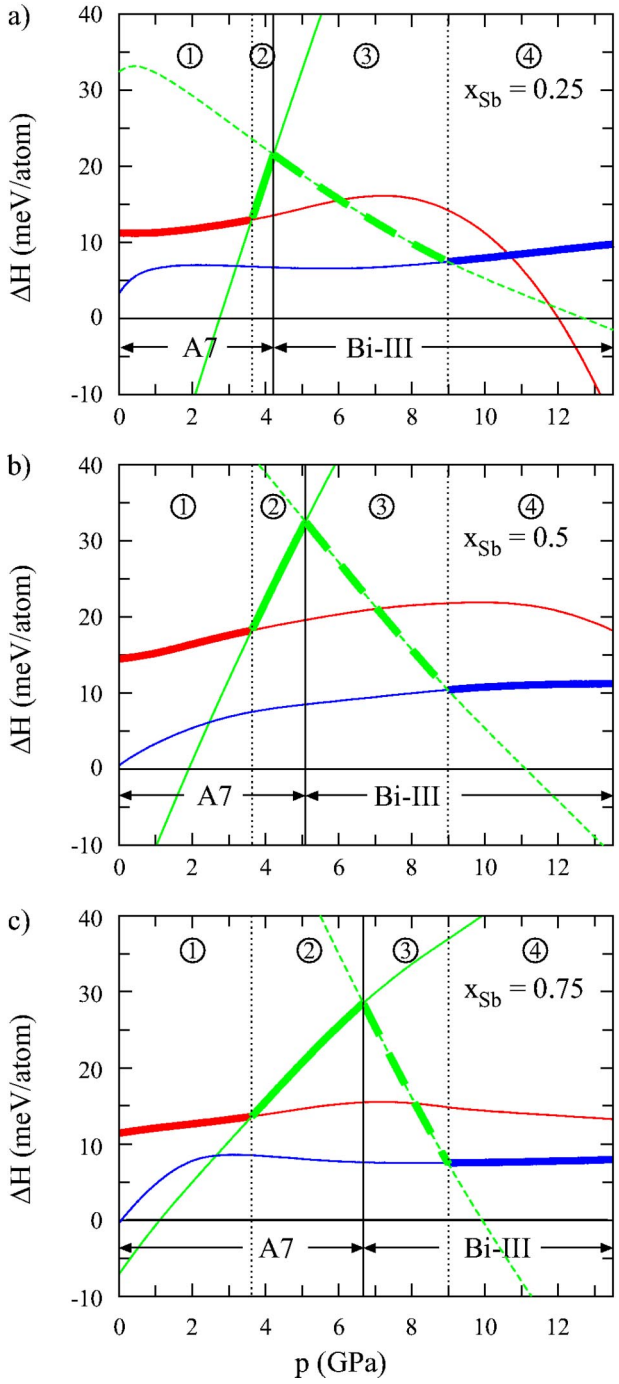

FIG. 10. (Color online) Calculated enthalpy differences ΔH as a function of pressure for the reactions: (1) $(1-x)$Bi(A7)$+x$Sb(A7) $\rightarrow$$Bi_{1-x}Sb_x$(A7) (red); (2) $(1-x)$Bi(Bi-III)$+x$Sb(A7) $\rightarrow$$Bi_{1-x}Sb_x$(A7) (green); (3) $(1-x)$Bi(Bi-III)$+x$Sb(A7) $\rightarrow$$Bi_{1-x}Sb_x$(Bi-III) (green, dotted); and (4) $(1-x)$Bi(Bi-III) $+x$Sb(Bi-III)$\rightarrow$$Bi_{1-x}Sb_x$(Bi-III) (blue). Calculated transition pressures for Bi(A7)$\rightarrow$Bi(Bi-III) and Sb(A7)$\rightarrow$Sb(Bi-III) are marked by dotted vertical lines, and the one for $Bi_{1-x}Sb_x$(A7) $\rightarrow$$Bi_{1-x}Sb_x$(Bi-III) is marked by a solid vertical line. These transition pressures define the pressure regions (1)–(4) for the four reactions. (a) $x_{Sb}=0.25$, (b) $x_{Sb}=0.50$, (c) $x_{Sb}=0.75$.

indicated in Fig. 6 and ranges from $x_{Sb}=0.10$–0.20 to $x_{Sb}=0.80$–0.85 for pressures between 3 GPa (A7$\rightarrow$Bi-III transition pressure of the Bi-rich part) and 7 GPa (A7$\rightarrow$Bi-III transition pressure of the Sb-rich part). A second gap connected with the Bi-III$\rightarrow$bcc transition might exist at higher pressures.

V. SUMMARY

We performed a combined experimental and calculational investigation of the high-pressure behavior of $Bi_{1-x}Sb_x$ alloys. These alloys, as well as the underlying elements Bi and Sb, possess the A7 structure as ground-state structure. Bi and Sb transform into a peculiar incommensurate composite structure under pressure and our intention was to examine how this incommensuration is influenced when two differently sized elements in different concentration form the composite structure. Our investigation was obscured by the occurrence of a phase separation which accompanied the transition A7$\rightarrow$Bi-III. Structural parameters of phases with the Bi-III composite structure are almost unaffected by pressure and composition effects. Most likely, Bi and Sb atoms are randomly distributed on the host and guest sublattices of this structure. From theoretical calculations we could show that alloys $Bi_{1-x}Sb_x$ in both the ground-state A7 and the high-pressure composite structures are energetically unstable towards decomposition into the elements. The formation enthalpy takes a maximum value at a pressure corresponding to the alloy A7$\rightarrow$Bi-III transition, which explains the experimentally observed phase separations.

Most remarkable is the finding that the incommensuration of the Bi-III structure is virtually not influenced by either composition and pressure. The fact that this structure is site-disordered in alloys $Bi_{1-x}Sb_x$ supports the finding from previous electronic structure calculations that the host and guest components are not really electronically different.[32] In particular, the intuitive picture of differently charged or polarized host and guest atoms is neither supported by theory (i.e., the partial DOS of the host and guest components are very similar[32]) nor by experiment (i.e., a segregation of Sb and Bi on the different components is not observed). For the group 15 elements the electronic structure changes accompanying the A7 $\rightarrow$ Bi-III transition are smooth. The persistence of a *p* band bonding-antibonding splitting in the electronic structure of materials with the Bi-III structure indicates still significant covalent *p*-*p* bonding. In recent articles we therefore argued that the Bi-III structure is a consequence of a delicate interplay between the electrostatic and the band energy contribution to the total energy.[32,36] In the intermediate pressure range of heavier group 15 elements both important parts of the total energy account equally for structural stability.

ACKNOWLEDGMENTS

This work was supported by the Carl Trygger Foundation, the Swedish National Research Council (VR), and SSF. O.D. acknowledges an EPSRC Studentship and a UK Scholarship for International Research Students.

[1] U. Schwarz, A. Grzechnik, K. Syassen, I. Loa, and M. Hanfland, Phys. Rev. Lett. **83**, 4085 (1999); M.I. McMahon, S. Rekhi, and R.J. Nelmes, *ibid.* **87**, 055501 (2001).
[2] R.J. Nelmes, D.R. Allan, M.I. McMahon, and S.A. Belmonte, Phys. Rev. Lett. **83**, 4081 (1999).
[3] M.I. McMahon, T. Bovornratanaraks, D.R. Allan, S.A. Belmonte, and R.J. Nelmes, Phys. Rev. B **61**, 3135 (2000).
[4] M.I. McMahon, O. Degtyareva, and R.J. Nelmes, Phys. Rev. Lett. **85**, 4896 (2000).
[5] V. Heine, Nature (London) **403**, 836 (2000).
[6] J. Donohue, *The Structures of the Elements* (Wiley, New York, 1974).
[7] P.W. Bridgman, Proc. Am. Acad. Arts Sci. **74**, 425 (1942).
[8] H. Iwasaki and T. Kikegawa, High Press. Res. **6**, 121 (1990).
[9] K. Aoki, S. Fujiwara, and M. Kusakabe, Solid State Commun. **45**, 161 (1983).
[10] P.W. Bridgman, Phys. Rev. **48**, 893 (1935).
[11] R.M. Brugger, R.B. Bennion, and T.G. Walton, Phys. Lett. **24A**, 714 (1967).
[12] J.H. Chen, H. Iwasaki, and T. Kikegawa, High Press. Res. **15**, 143 (1996).
[13] K. Aoki, S. Fujiwara, and M. Kusakabe, J. Phys. Soc. Jpn. **51**, 3826 (1982).
[14] Each net atom forms part of three triangles (3) and two squares (4) arranged in the sequence ''33434'' around the atom [see, e.g., W. B. Pearson, *The Crystal Chemistry and Physics of Metals and Alloys* (Wiley, New York, 1972)].
[15] P.W. Bridgman, Proc. Am. Acad. Arts Sci. **84**, 43 (1955).
[16] M. Akaishi and S. Saito, Bull. Tokyo Inst. Technol. **120**, 81 (1974).
[17] T.N. Kolobyanina, S.S. Kabalkina, L.F. Verezhagin, A.Ya. Michkov, and M.F. Kachan, Zh. Eksp. Teor. Fiz. **59**, 1146 (1970) [Sov. Phys. JETP **32**, 624 (1971)].
[18] W.F. Ehret and M.B. Abramson, J. Am. Chem. Soc. **56**, 385 (1934).
[19] P.-E. Werner, Ark. Kemi **31**, 513 (1969).
[20] R.J. Nelmes and M.I. McMahon, J. Synchrotron Radiat. **1**, 69 (1994).
[21] G.J. Piermarini, S. Block, J.D. Barnett, and R.A. Forman, J. Appl. Phys. **46**, 2774 (1975).
[22] V. Petricek and M. Dusek, *The Crystallographic Computing System* JANA200 (Institute of Physics, Praha, Czech Republic, 2000).
[23] M.I. McMahon, O. Degtyareva, C. Hejny, and R.J. Nelmes, High Press. Res. **23**, 289 (2003).
[24] M. I. McMahon, O. Degtyareva, R. J. Nelmes, S. van Smaalen, and L. Palatinus (unpublished).
[25] A differently modulated structure extracted from powder data was recently reported for Sb-II (Ref. 26).
[26] U. Schwarz, L. Akselrud, H. Rosner, Alim Ormeci, and Yu. Grin, Phys. Rev. B **67**, 214101 (2003).
[27] *International Tables for Crystallography*, edited by A. J. C. Wilson, Mathematical, Physical and Chemical Tables, Vol. C (Kluwer Academic, Dordrecht, 1995).
[28] P.E. Blöchl, Phys. Rev. B **50**, 17 953 (1994); G. Kresse and J. Joubert, *ibid.* **59**, 1758 (1999).
[29] G. Kresse and J. Hafner, Phys. Rev. B **47**, 558 (1993); G. Kresse and J. Furthmüller, *ibid.* **54**, 11 169 (1996).
[30] J.P. Perdew and Y. Wang, Phys. Rev. B **45**, 13 244 (1992).
[31] H.J. Monkhorst and J.D. Pack, Phys. Rev. B **13**, 5188 (1976).
[32] U. Häussermann, K. Söderberg, and R. Norrestam, J. Am. Chem. Soc. **124**, 15 359 (2002).
[33] A. Zunger, S.H. Wei, L.G. Ferreira, and J.E. Bernard, Phys. Rev. Lett. **65**, 353 (1990).
[34] It was not possible to obtain phase compositions in multiphase specimens from the structure refinement procedure because of too severe correlations between scale factors and compositions and/or occupation parameters. The close similarity between the shape of the scattering curves of Bi and Sb (Ref. 27) will then imply that the structure of a single phase in a multiphase specimen can be refined equally well, with any linear combination of scattering factors. Phase fractions were refined with a fixing the phase compositions at the values obtained from the estimation performed according to Fig. 2.
[35] *Gmelins Handbuch der Anorganischen Chemie, Wismut Ergänzungsband, 8. Auflage* (Verlag Chemie, Weinheim, 1964).
[36] U. Häussermann, Chem.-Eur. J. **9**, 1471 (2003).
[37] This information can be obtained at http://www.fos.su.se/~rolf/bisb_2003.pdf